10.1071/CH14390_AC

Australian Journal of Chemistry **2014, 67(11), 1618-1624**

SUPPLEMENTARY MATERIAL

Manganese(II) Oxazolidine Nitroxide Chelates; Structure, Magnetism and Redox Properties

Ian A. Gass,[A,B] *Mousa Asadi,* [A] *David W. Lupton,*[A] *Boujemaa Moubaraki,*[A] *Alan M. Bond,*[A]

Si-Xuan Guo, [A] *and Keith S. Murray.*[A,C]*

[A]School of Chemistry, Monash University, Clayton, Victoria 3800, Australia
[B]Present address: School of Pharmacy and Biomolecular Sciences, University of Brighton, Brighton BN2 4GJ, UK
[C]Corresponding author. Email keith.murray@monash.edu

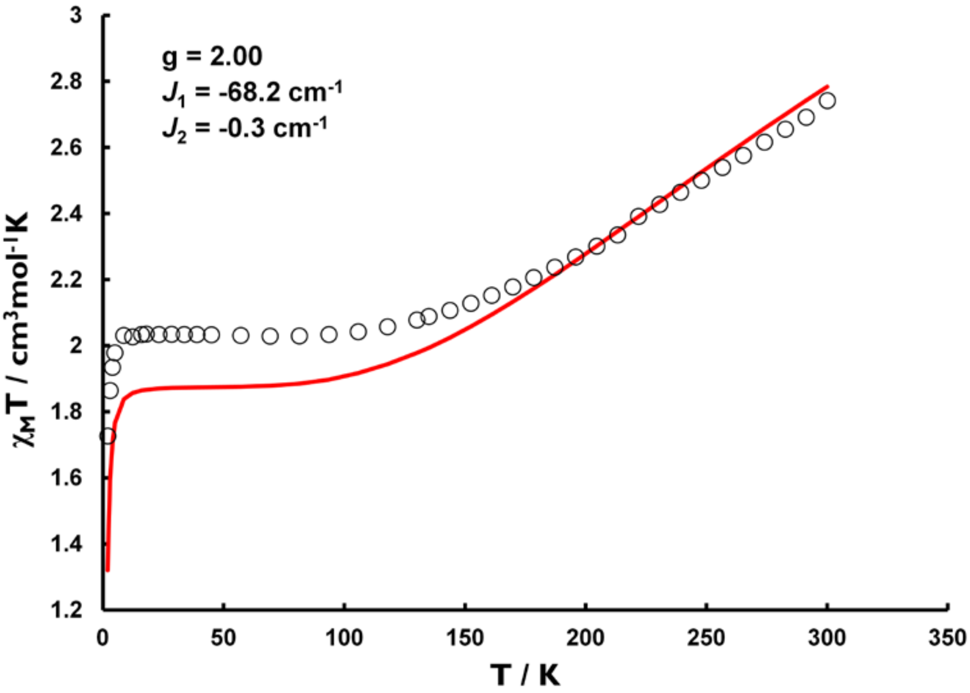

Figure S1. Plot of $\chi_M T$ vs T for **1** and best fit (red lines) with values shown inset.

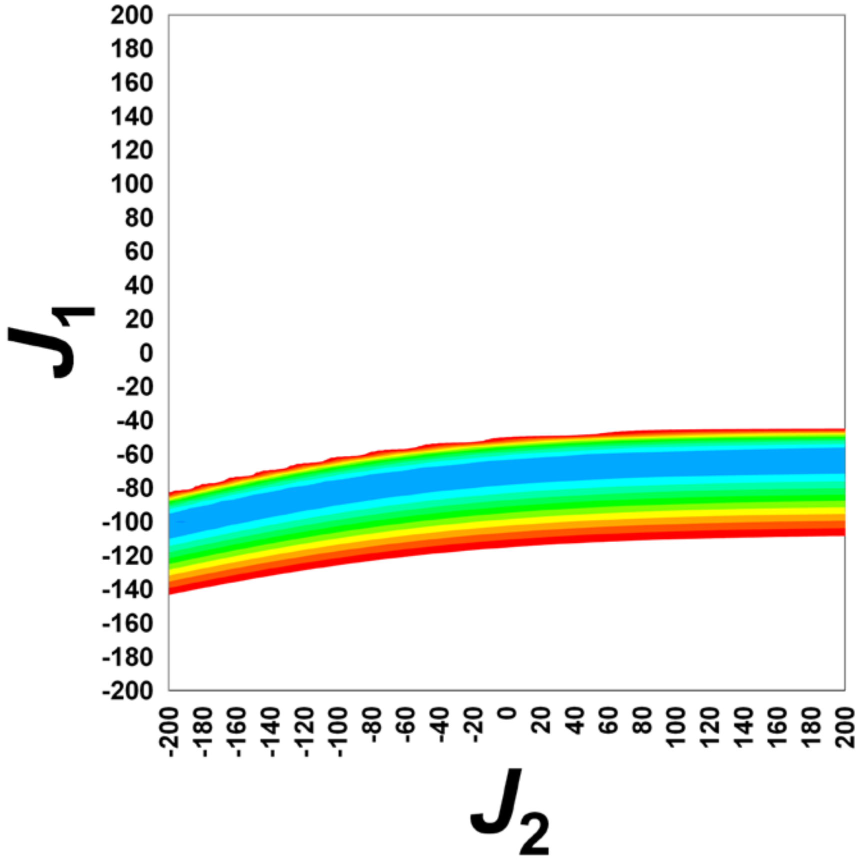

Figure S2. Contour plot of J_1 vs J_2 in cm^{-1} for complex **1** with lowest residual in blue with a fixed value of g = 2.00. Residual value capped at 3.9.

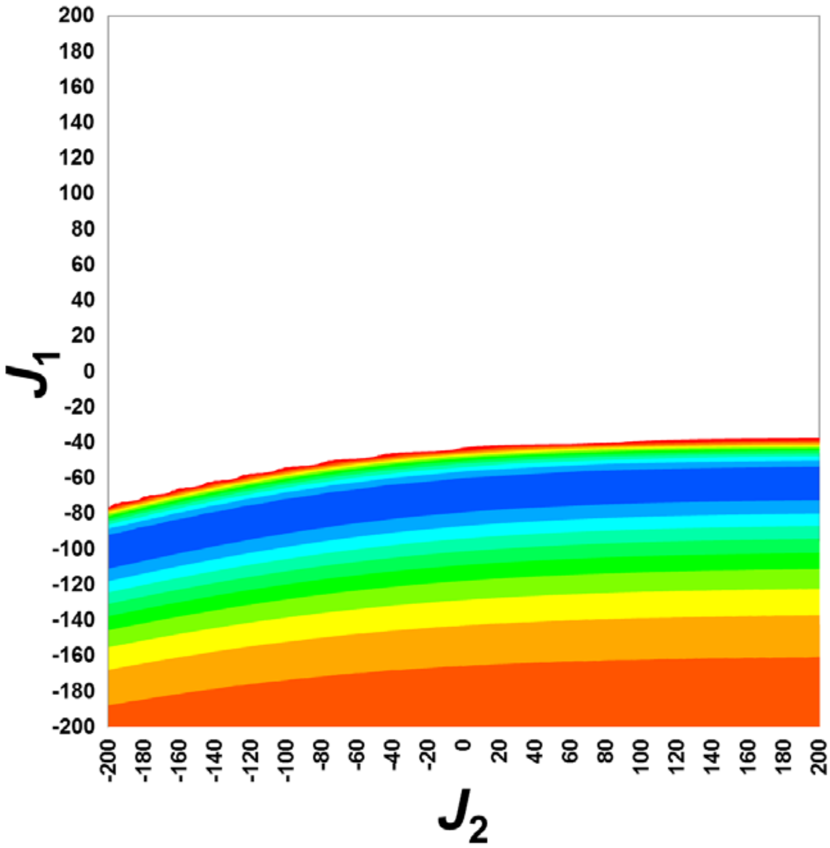

Figure S3. Contour plot of J_1 vs J_2 in cm^{-1} for complex **1** with lowest residual in blue with a fixed value of g = 2.00. Residual value capped at 7.8.

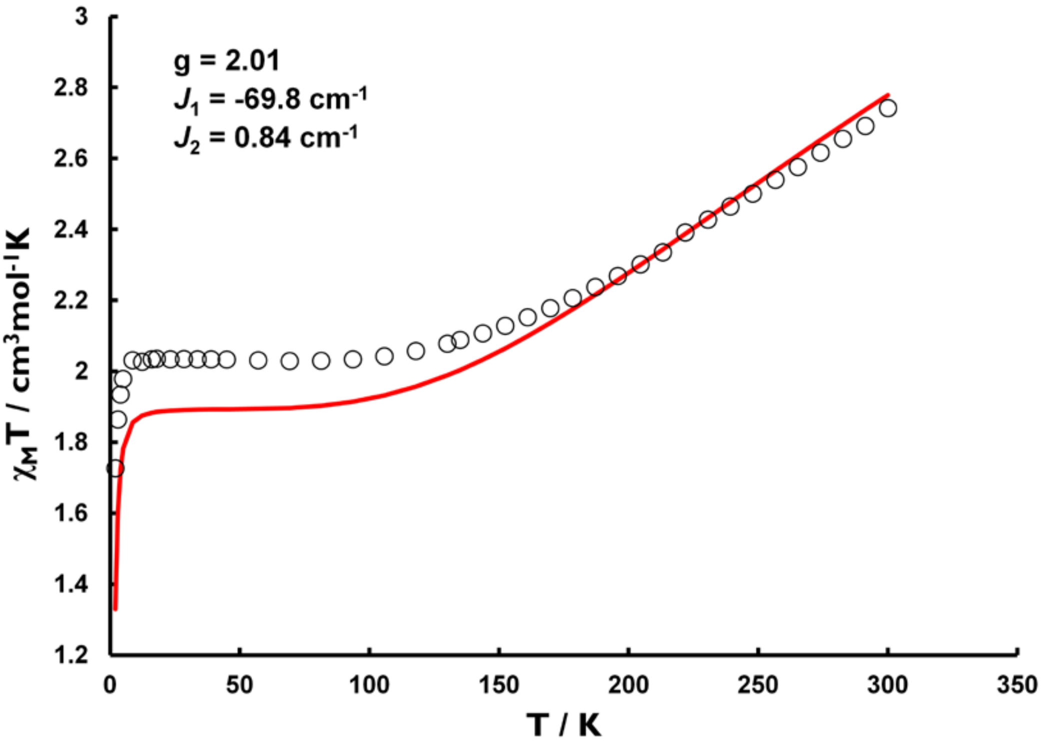

Figure S4. Plot of $\chi_M T$ vs T for **1** and best fit (red lines) with values shown inset.

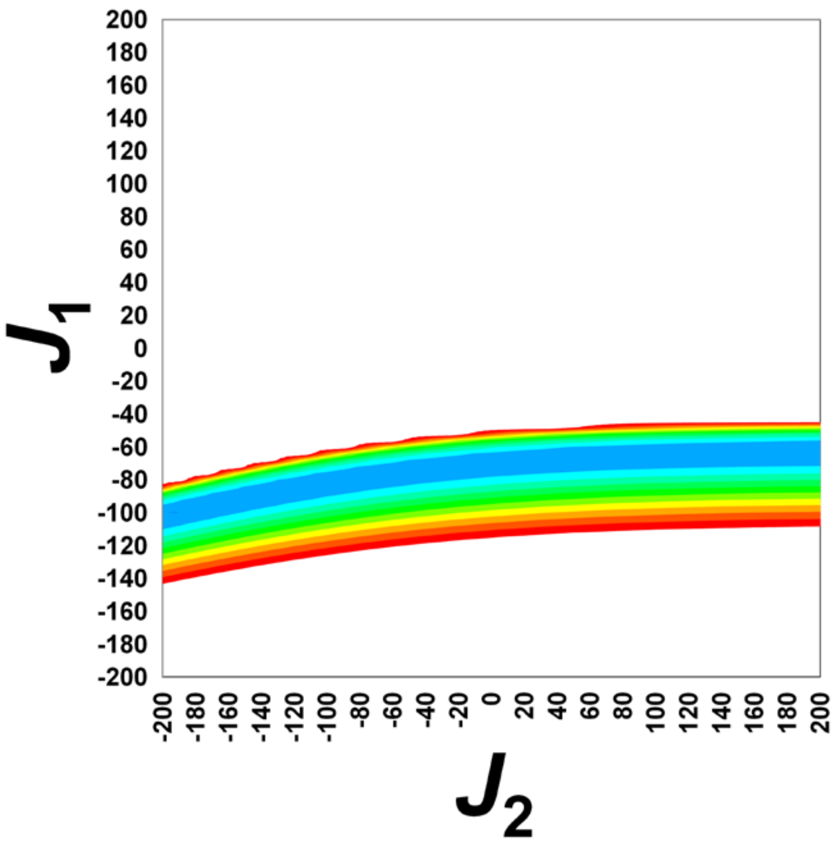

Figure S5. Contour plot of J_1 vs J_2 in cm^{-1} for complex **1** with lowest residual in blue with a fixed value of g = 2.01. Residual value capped at 3.9.

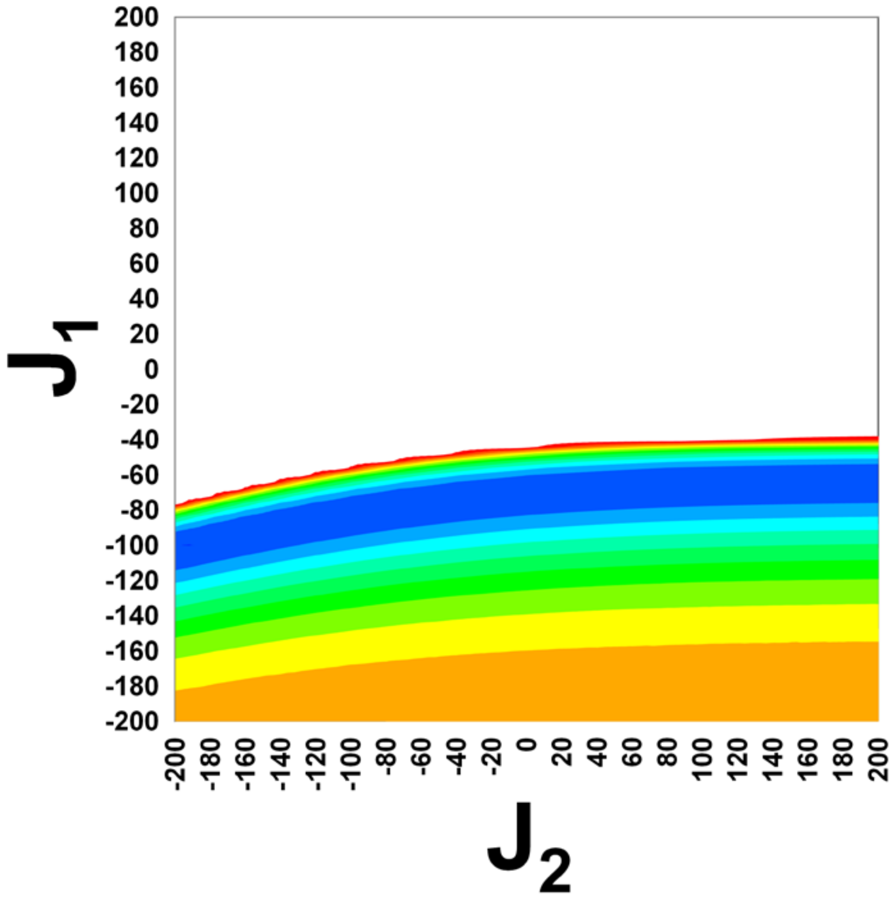

Figure S6. Contour plot of J_1 vs J_2 in cm^{-1} for complex **1** with lowest residual in blue with a fixed value of g = 2.01. Residual value capped at 7.8.

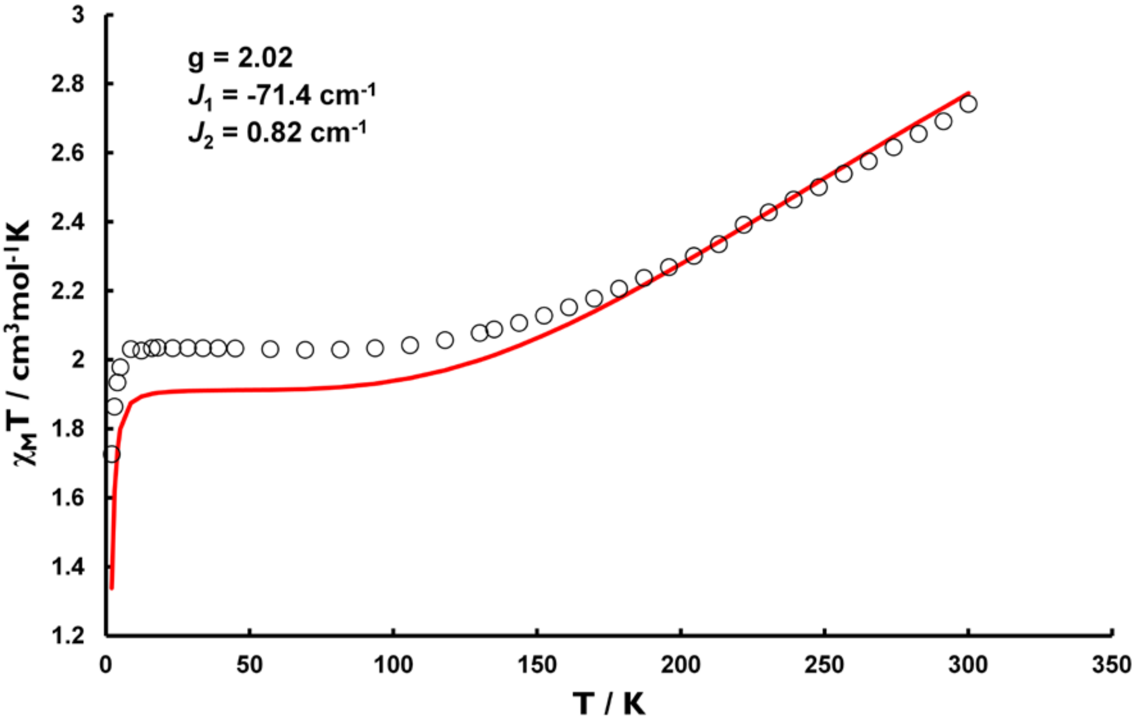

Figure S7. Plot of $\chi_M T$ vs T for **1** and best fit (red lines) with values shown inset.

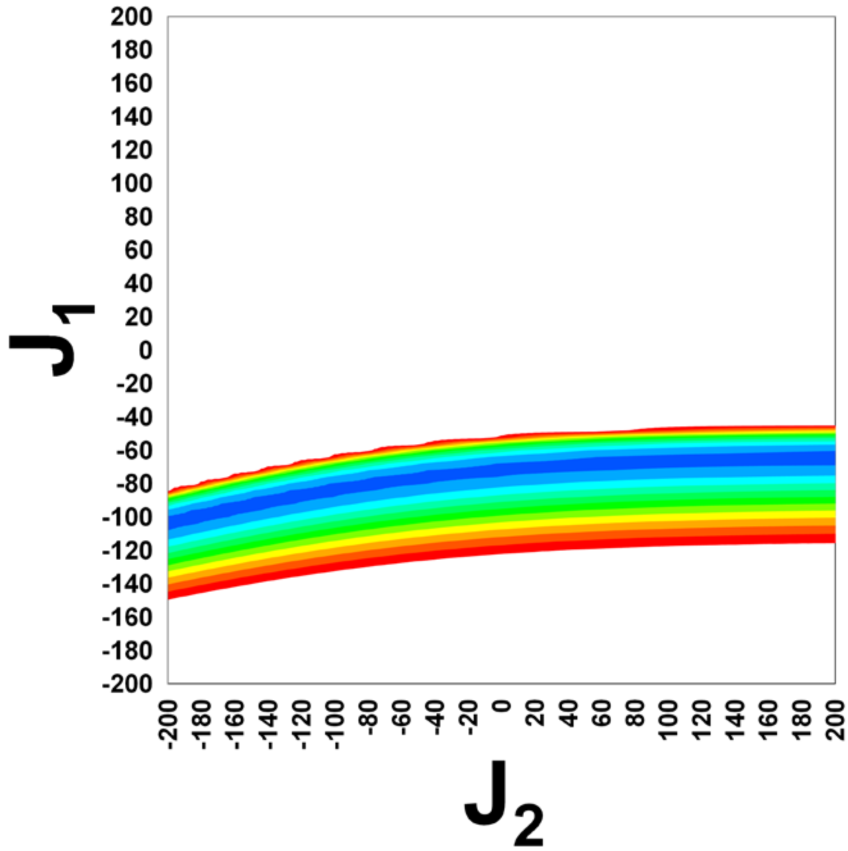

Figure S8. Contour plot of J_1 vs J_2 in cm^{-1} for complex **1** with lowest residual in blue with a fixed value of g = 2.02. Residual value capped at 3.9.

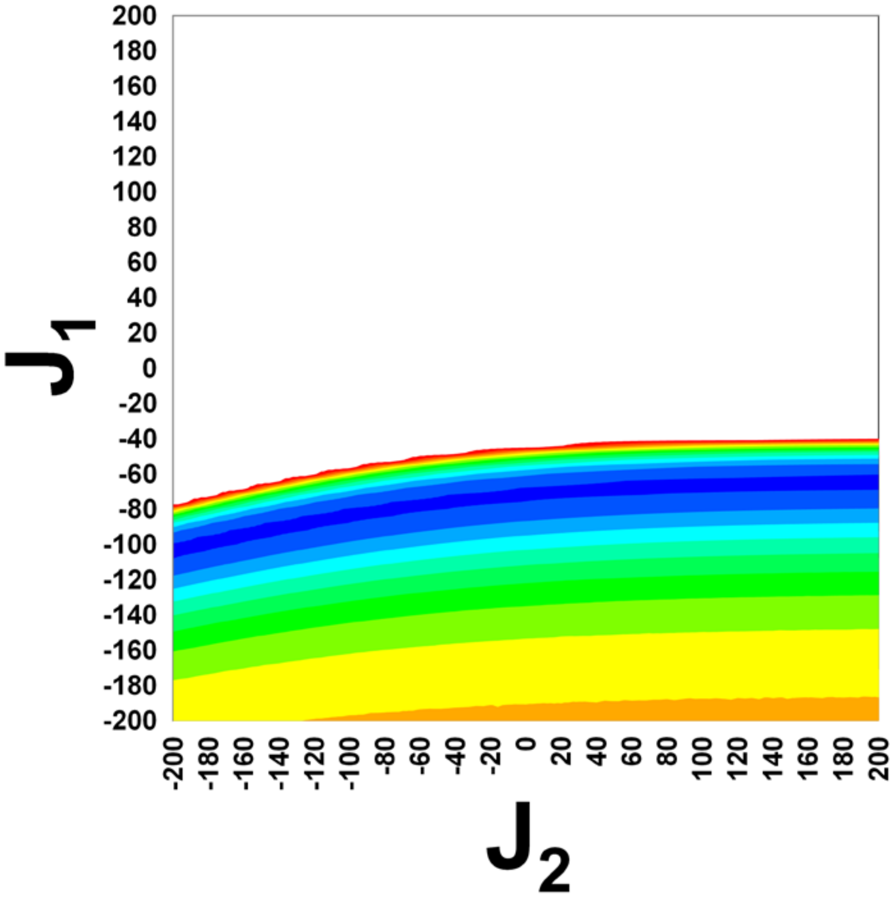

Figure S9. Contour plot of J_1 vs J_2 in cm^{-1} for complex **1** with lowest residual in blue with a fixed value of g = 2.02. Residual value capped at 7.8.

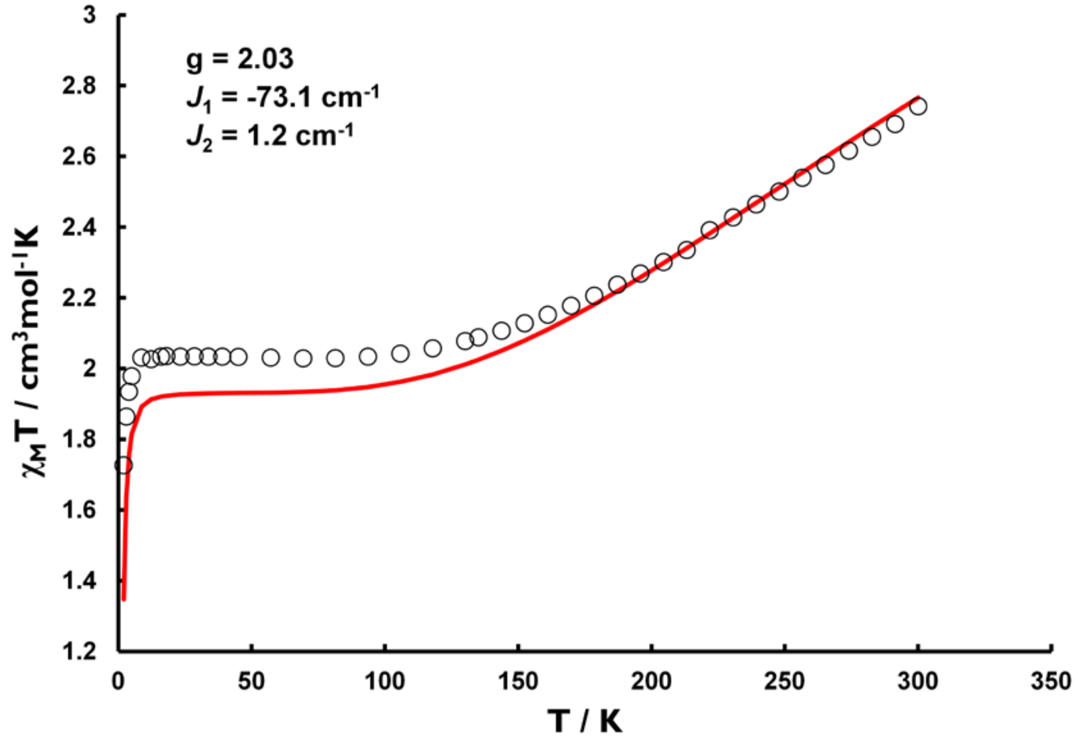

Figure S10. Plot of $\chi_M T$ vs T for **1** and best fit (red lines) with values shown inset.

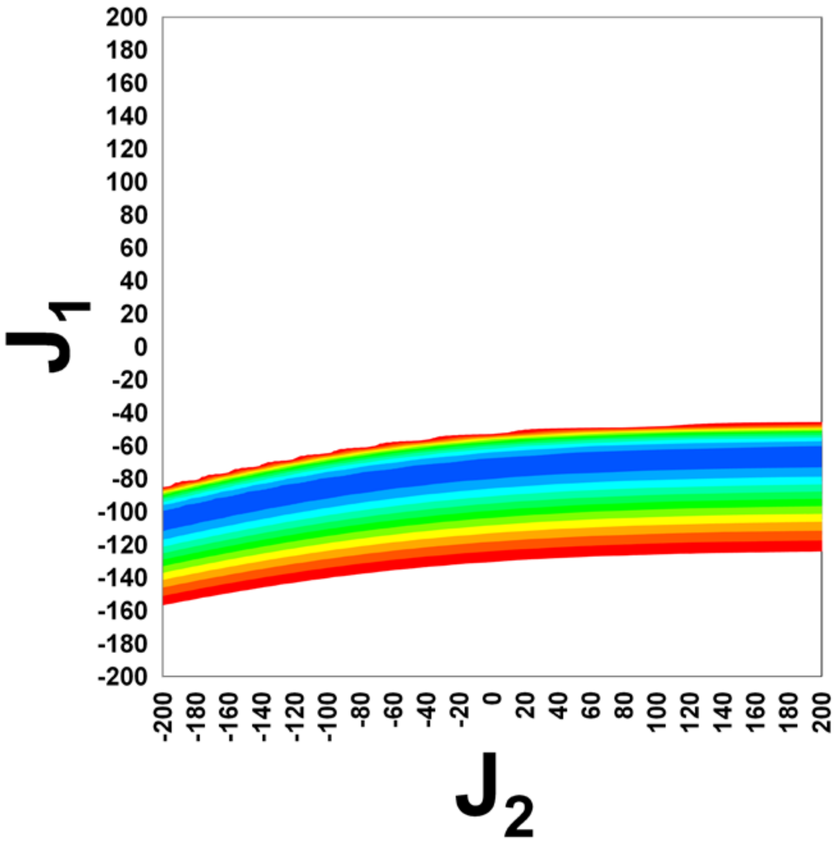

Figure S11. Contour plot of J_1 vs J_2 in cm^{-1} for complex **1** with lowest residual in blue with a fixed value of g = 2.03. Residual value capped at 3.9.

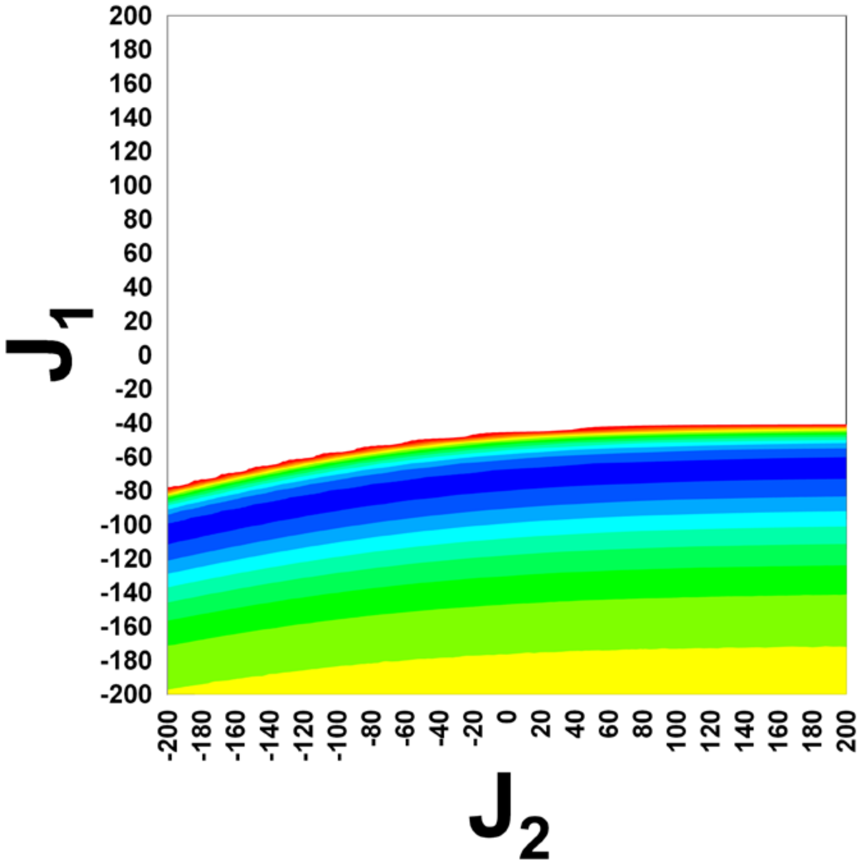

Figure S12. Contour plot of J_1 vs J_2 in cm^{-1} for complex **1** with lowest residual in blue with a fixed value of g = 2.03. Residual value capped at 7.8.

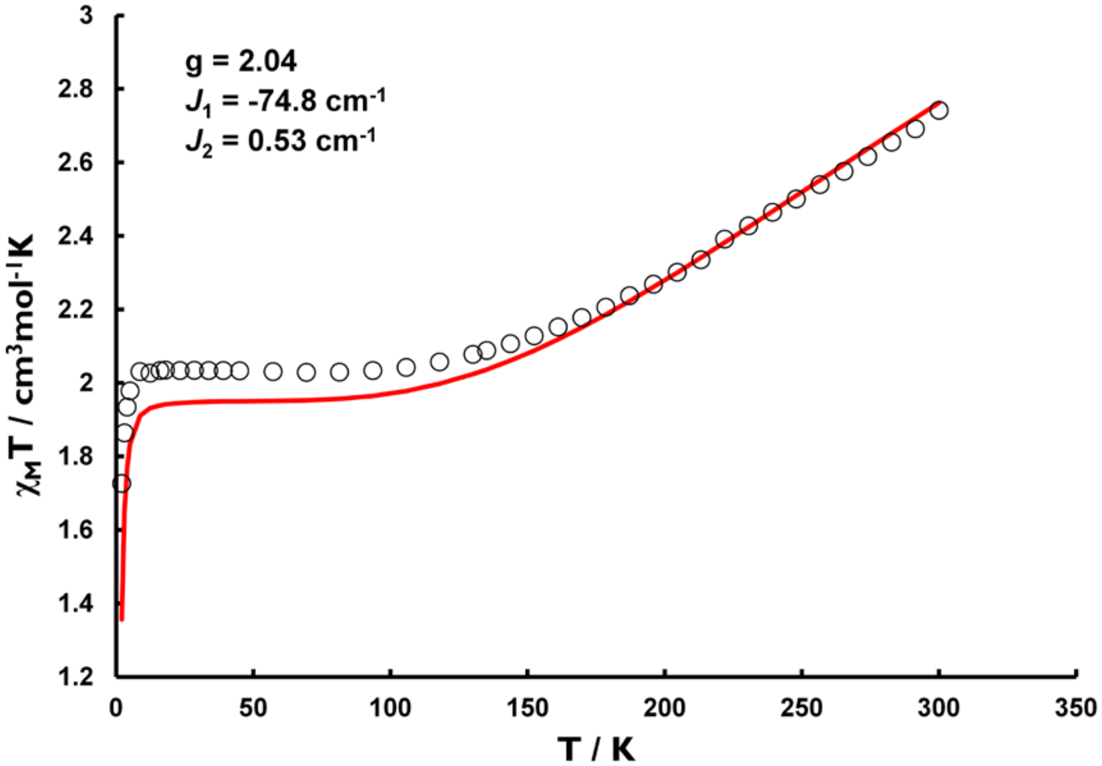

Figure S13. Plot of $\chi_M T$ vs T for **1** and best fit (red lines) with values shown inset.

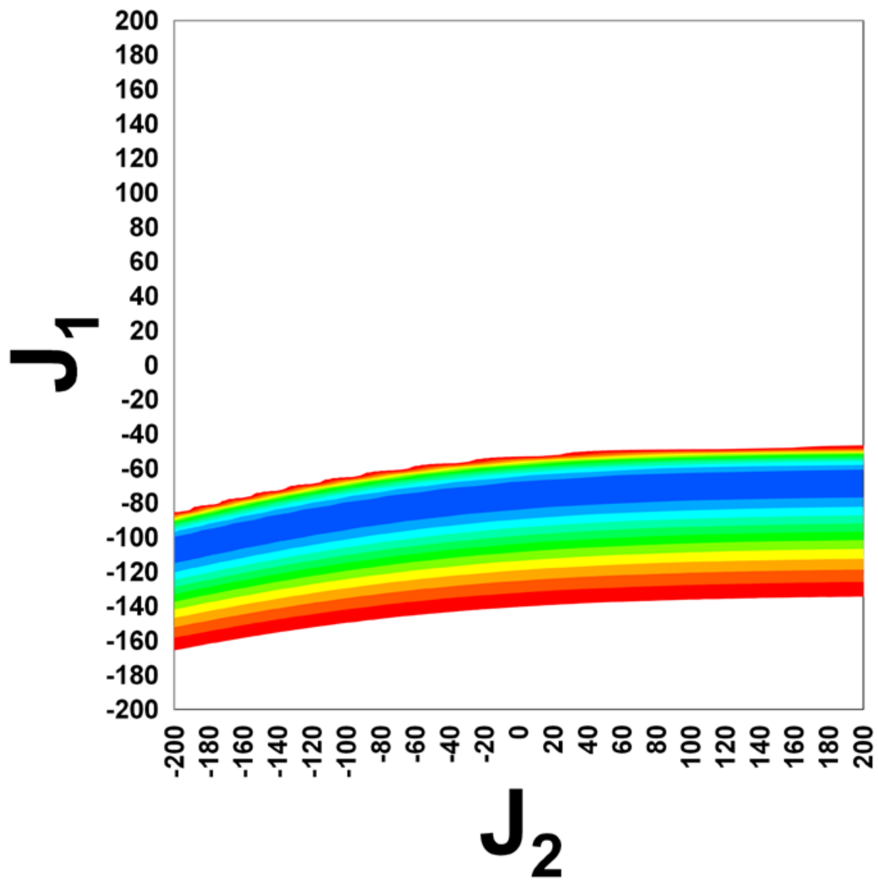

Figure S14. Contour plot of J_1 vs J_2 in cm^{-1} for complex **1** with lowest residual in blue with a fixed value of g = 2.04. Residual value capped at 3.9.

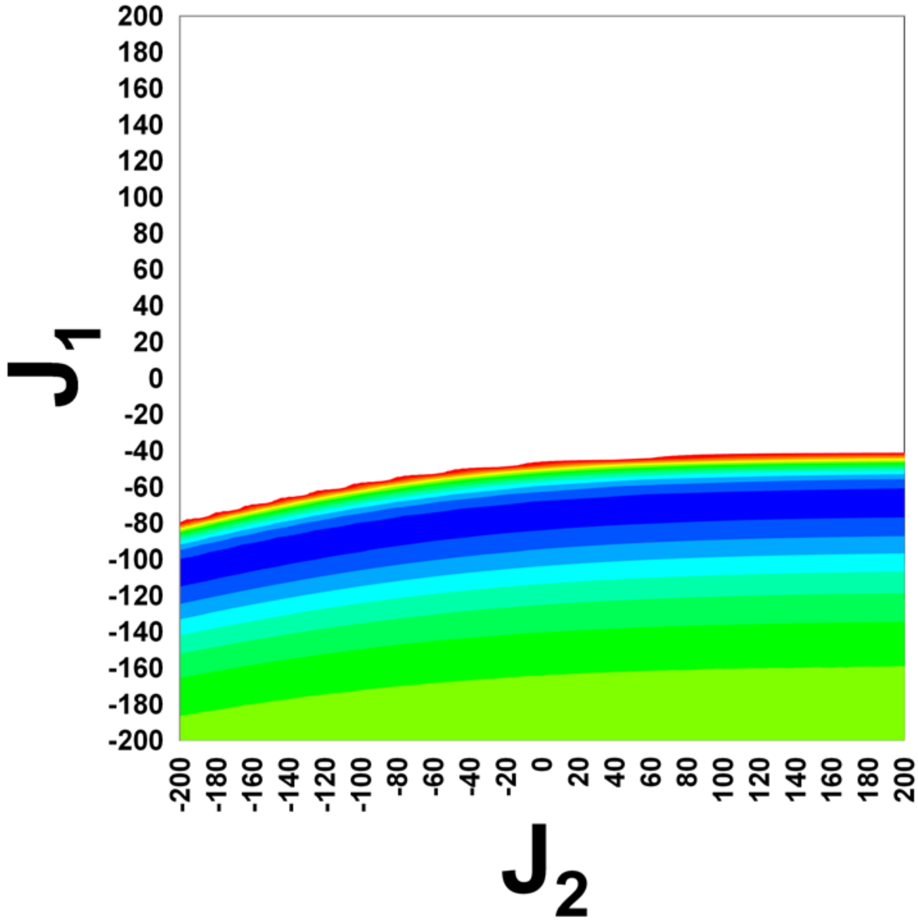

Figure S15. Contour plot of J_1 vs J_2 in cm^{-1} for complex **1** with lowest residual in blue with a fixed value of g = 2.04. Residual value capped at 7.8.

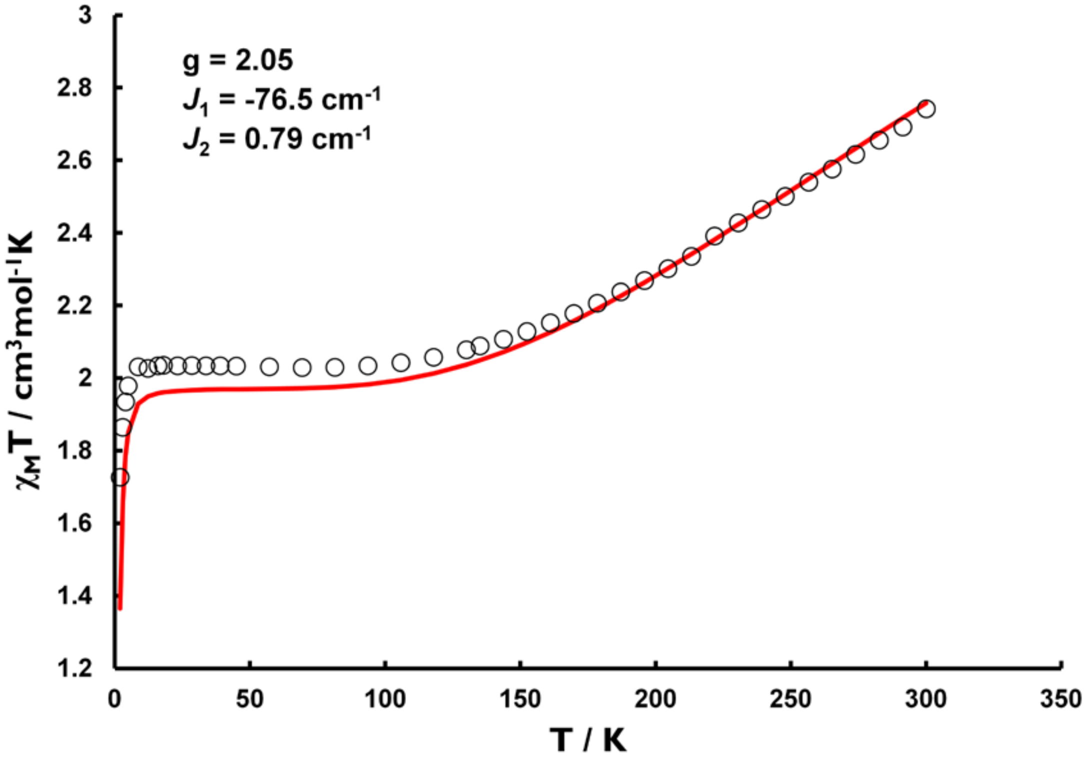

Figure S16. Plot of $\chi_M T$ vs T for **1** and best fit (red lines) with values shown inset.

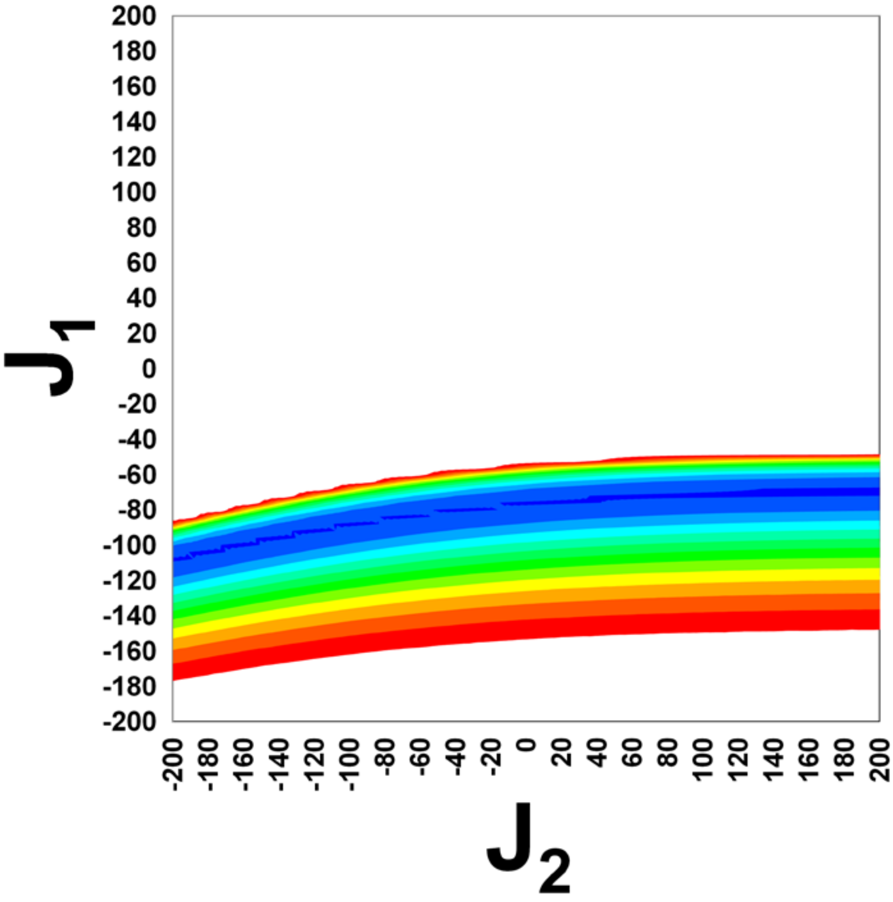

Figure S17. Contour plot of J_1 vs J_2 in cm^{-1} for complex **1** with lowest residual in blue with a fixed value of g = 2.05. Residual value capped at 3.9.

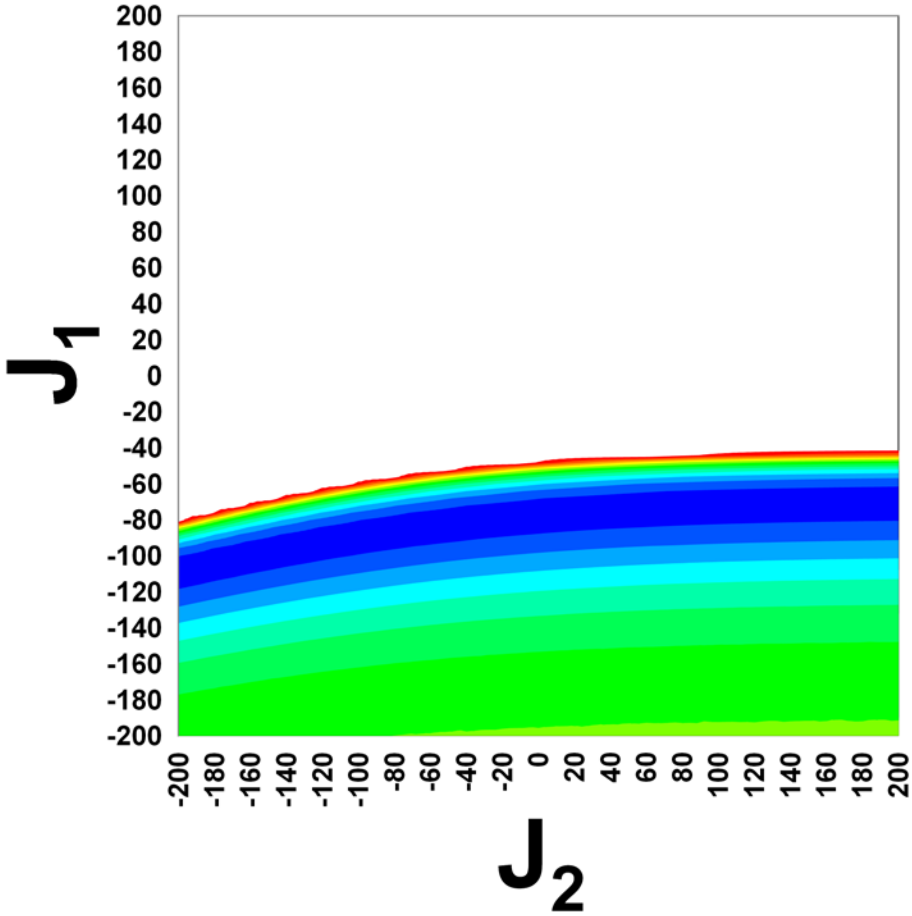

Figure S18. Contour plot of J_1 vs J_2 in cm^{-1} for complex **1** with lowest residual in blue with a fixed value of g = 2.05. Residual value capped at 7.8.

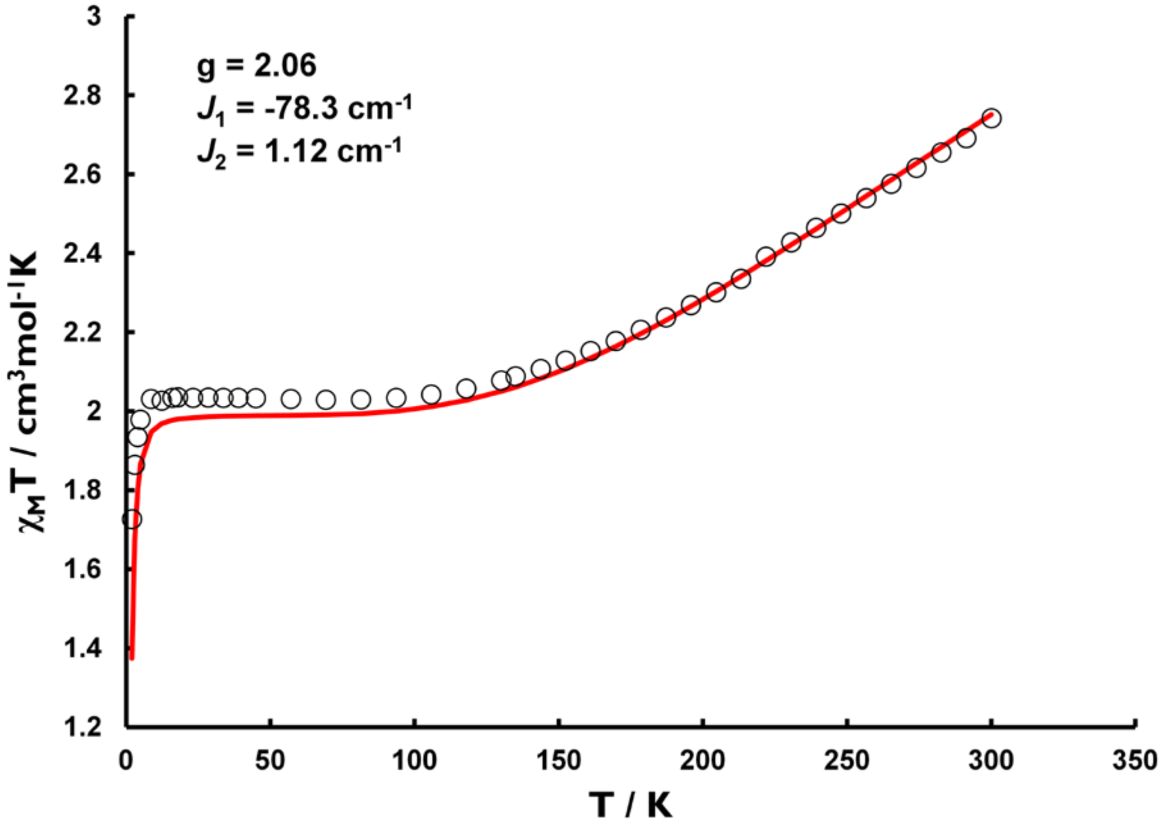

Figure S19. Plot of $\chi_M T$ vs T for **1** and best fit (red lines) with values shown inset.

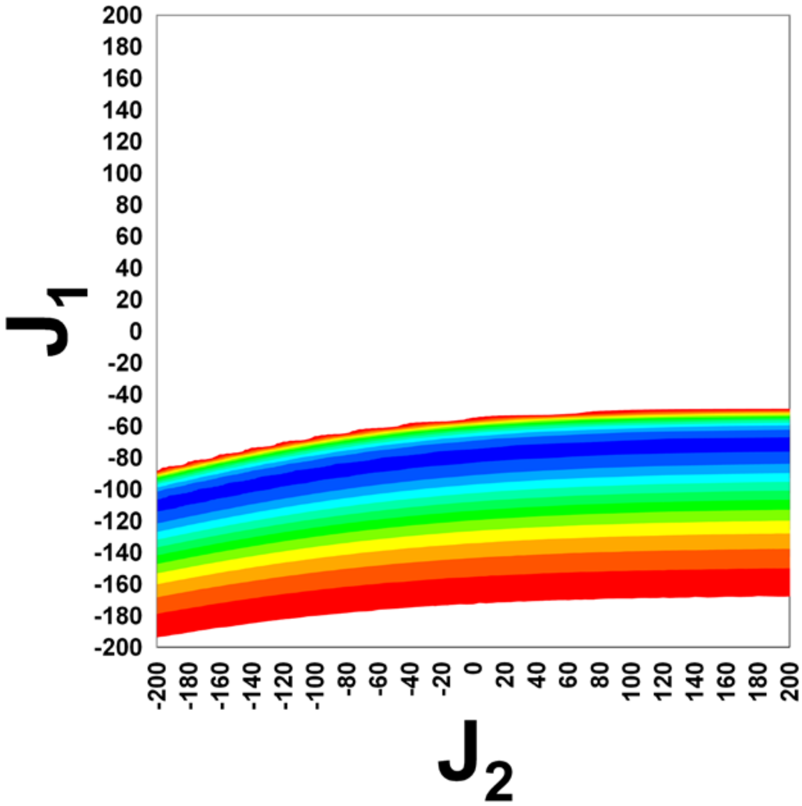

Figure S20. Contour plot of J_1 vs J_2 in cm^{-1} for complex **1** with lowest residual in blue with a fixed value of g = 2.06. Residual value capped at 3.9.

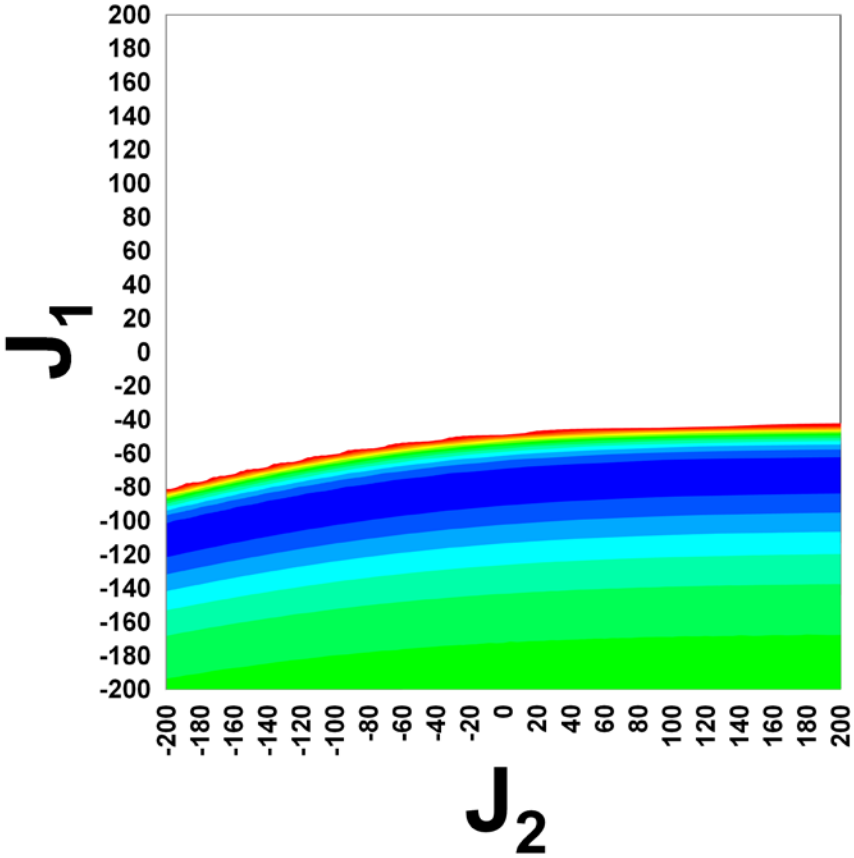

Figure S21. Contour plot of J_1 vs J_2 in cm^{-1} for complex **1** with lowest residual in blue with a fixed value of g = 2.06. Residual value capped at 7.8.

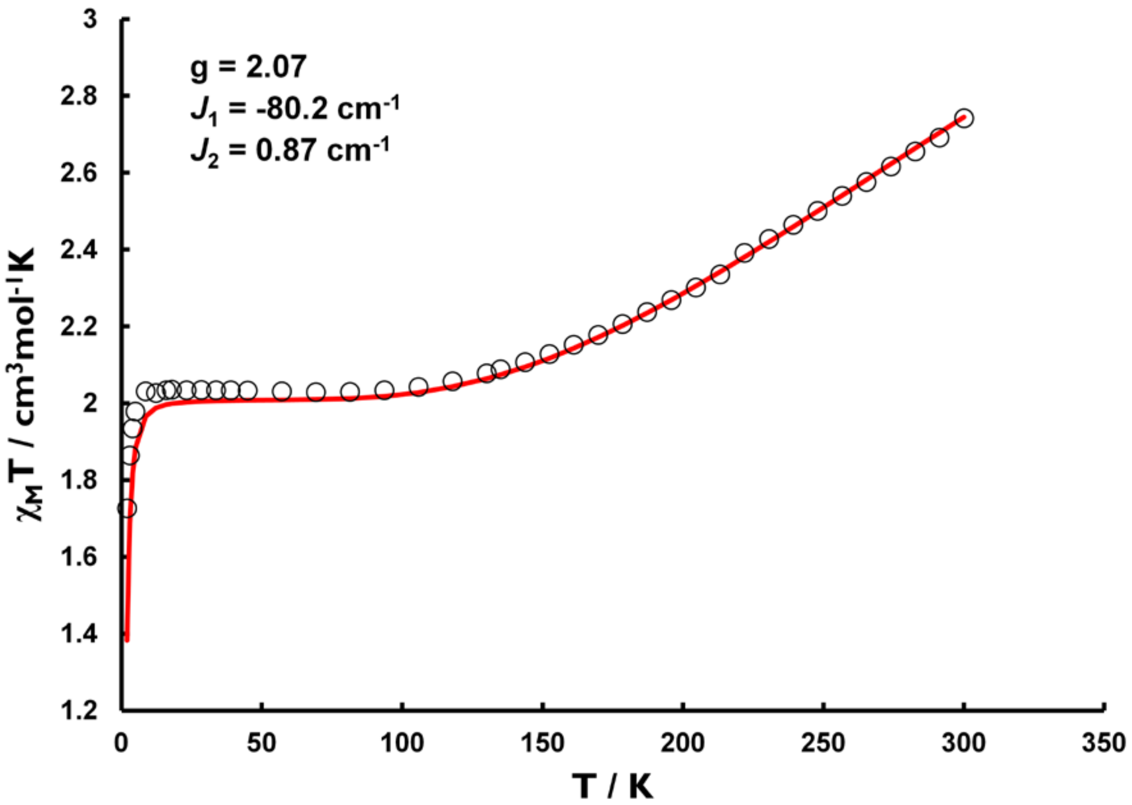

Figure S22. Plot of $\chi_M T$ vs T for **1** and best fit (red lines) with values shown inset.

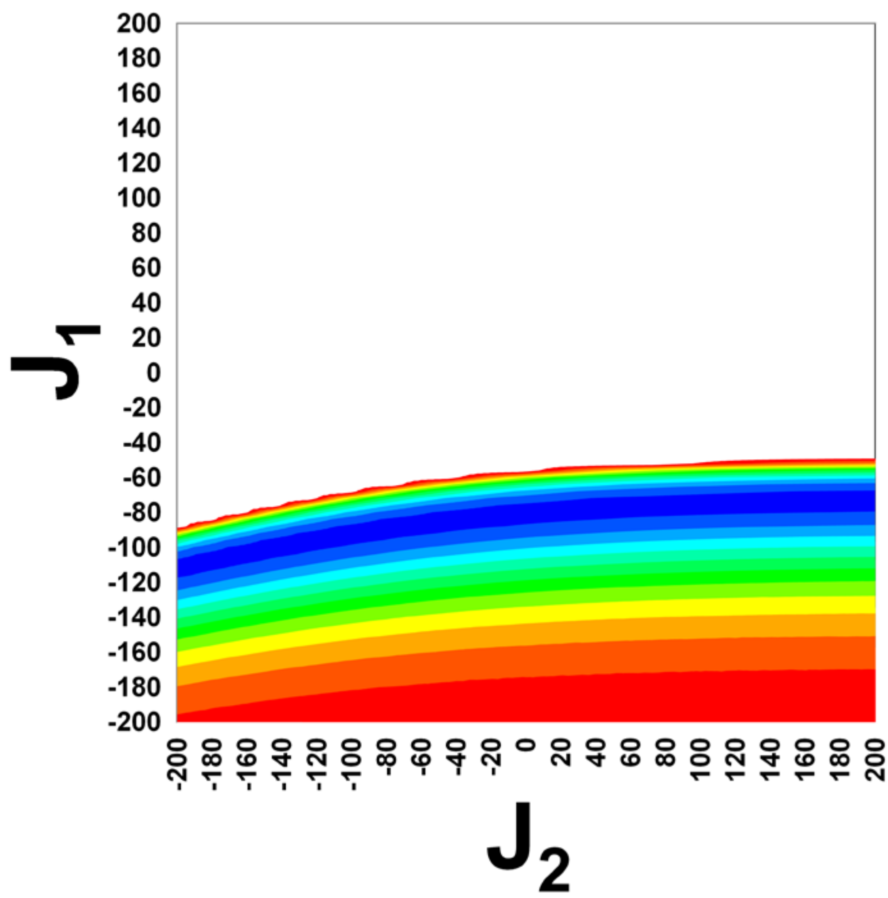

Figure S23. Contour plot of J_1 vs J_2 in cm^{-1} for complex **1** with lowest residual in blue with a fixed value of g = 2.07. Residual value capped at 3.9.

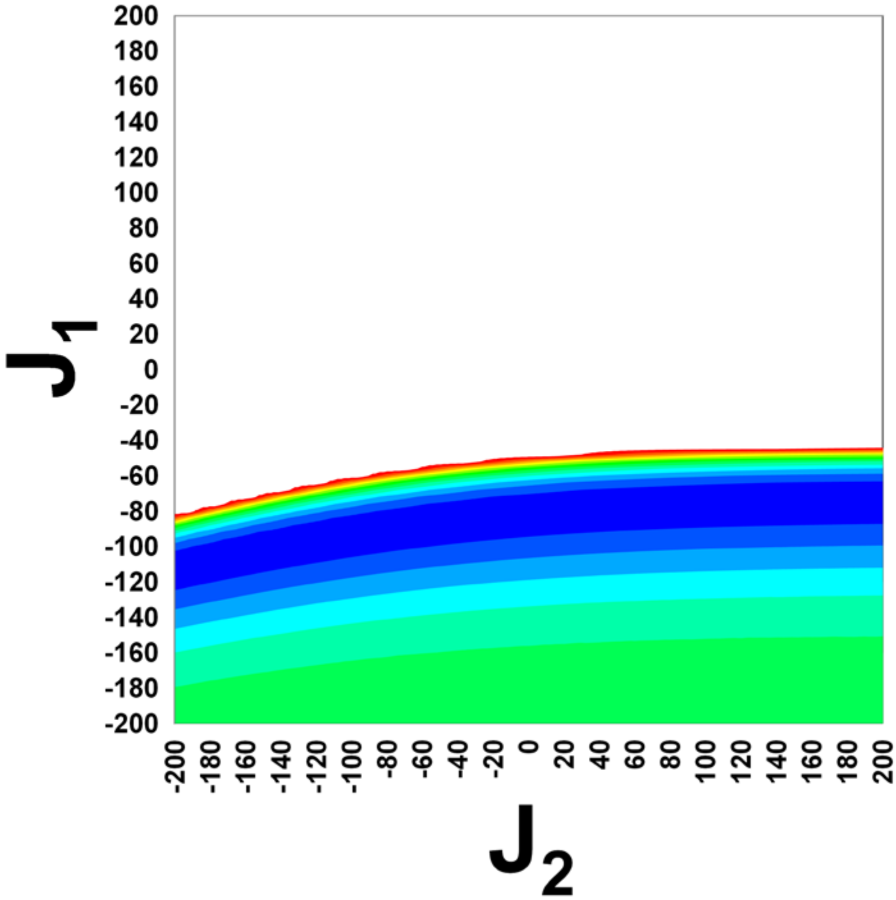

Figure S24. Contour plot of J_1 vs J_2 in cm^{-1} for complex **1** with lowest residual in blue with a fixed value of g = 2.07. Residual value capped at 7.8.

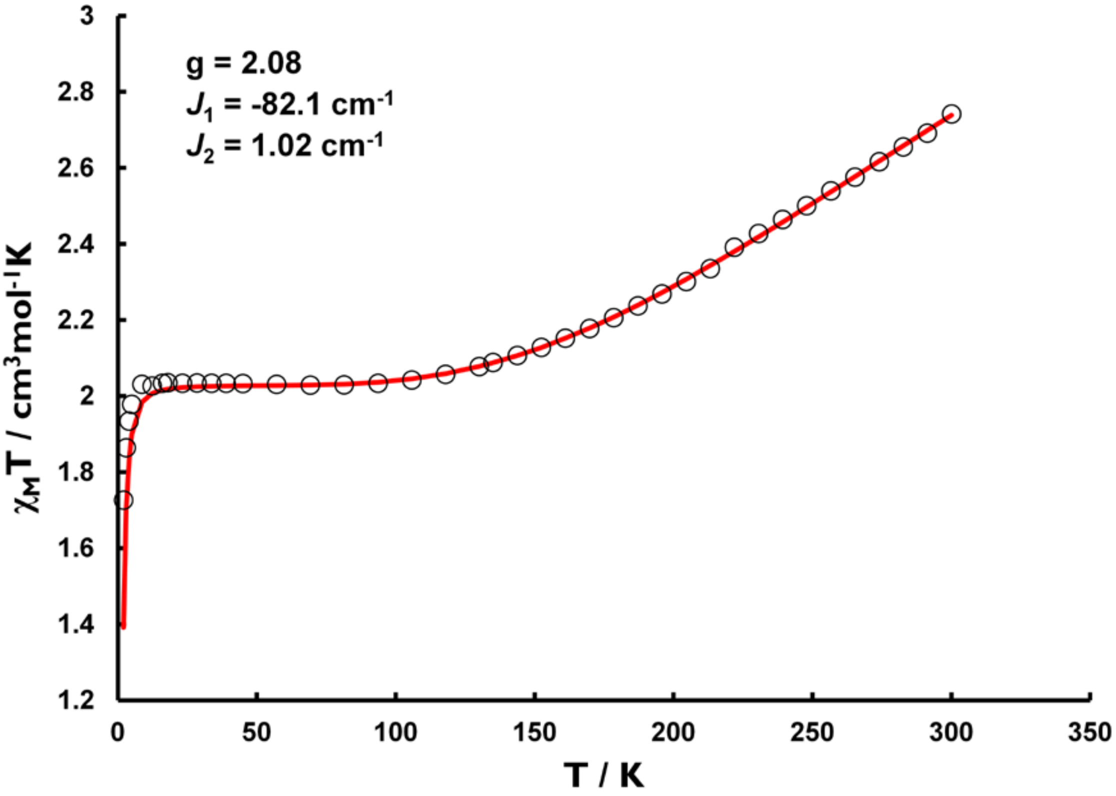

Figure S25. Plot of $\chi_M T$ vs T for **1** and best fit (red lines) with values shown inset.

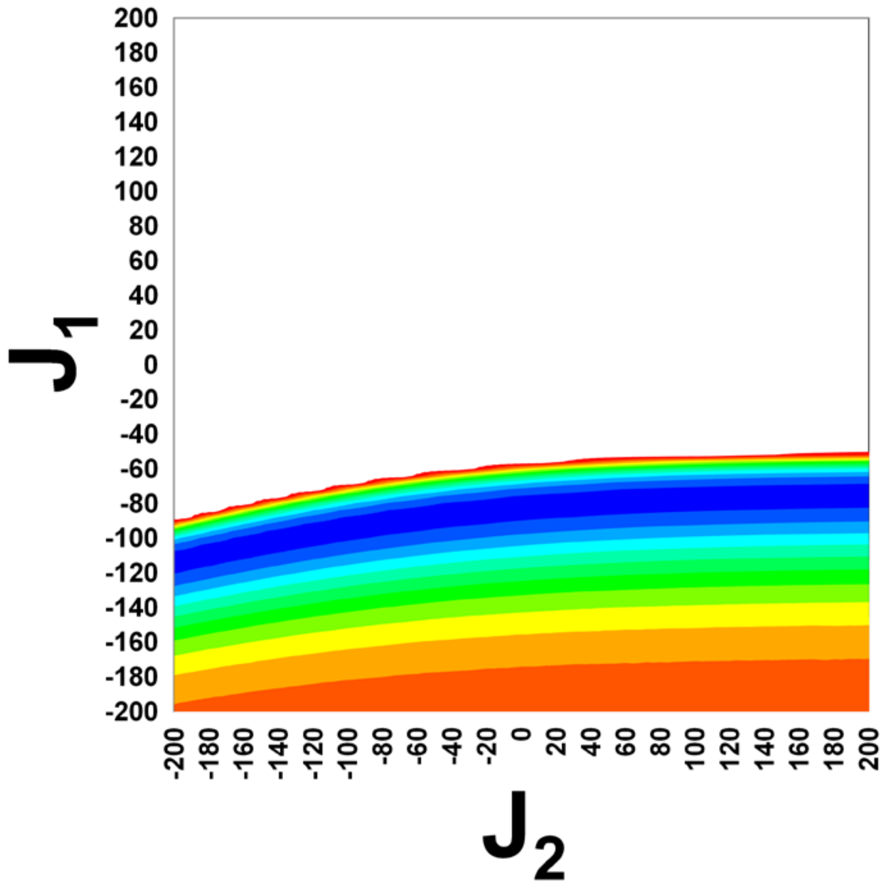

Figure S26. Contour plot of J_1 vs J_2 in cm^{-1} for complex **1** with lowest residual in blue with a fixed value of g = 2.08. Residual value capped at 3.9.

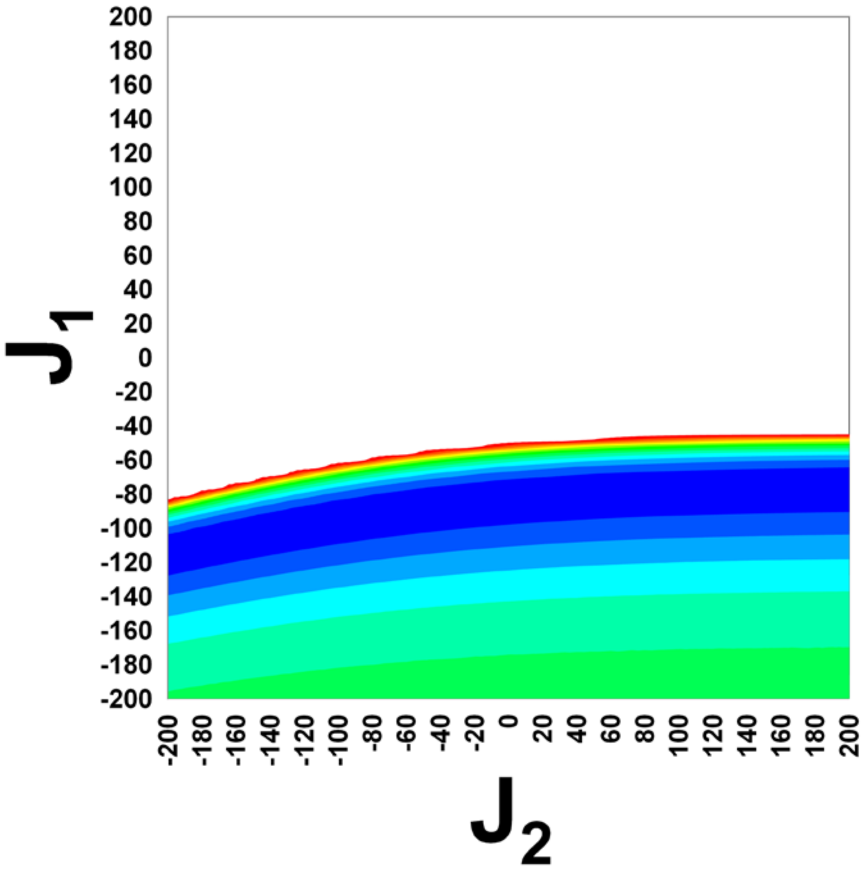

Figure S27. Contour plot of J_1 vs J_2 in cm^{-1} for complex **1** with lowest residual in blue with a fixed value of g = 2.08. Residual value capped at 7.8.

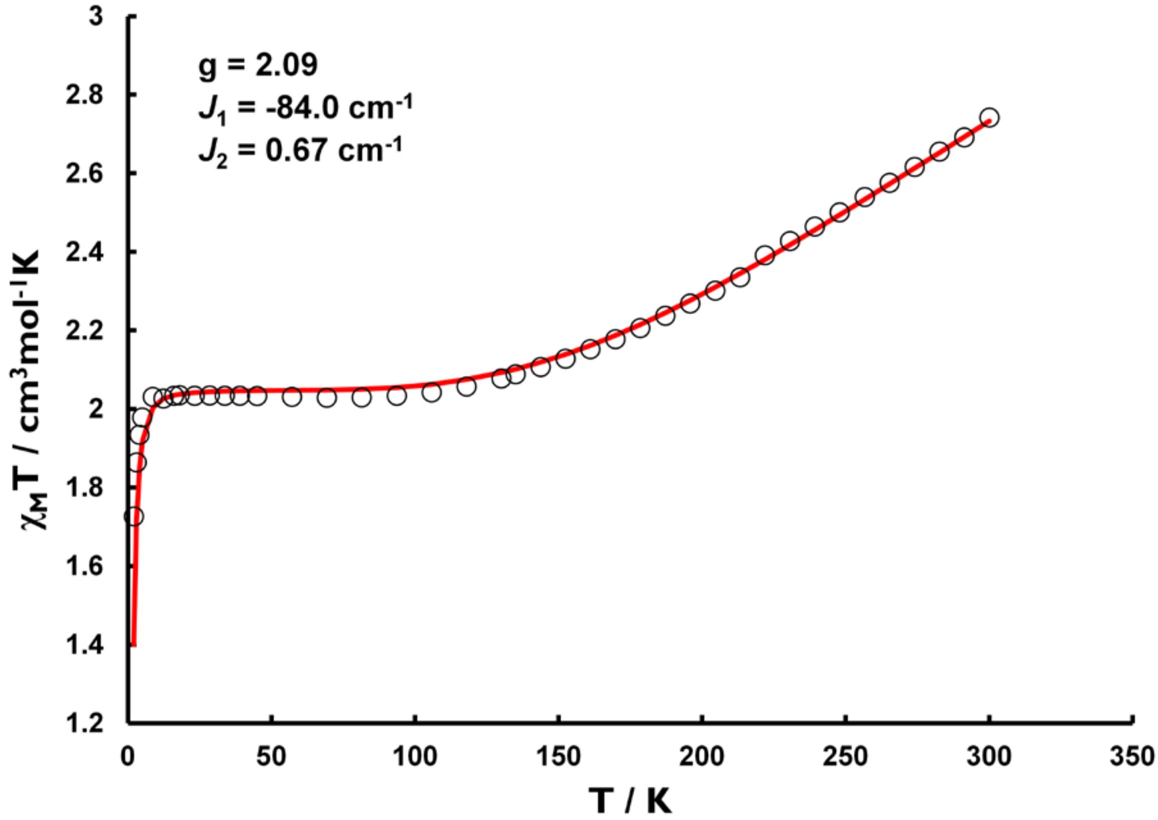

Figure S28. Plot of $\chi_M T$ vs T for **1** and best fit lines (red lines) with values shown inset.

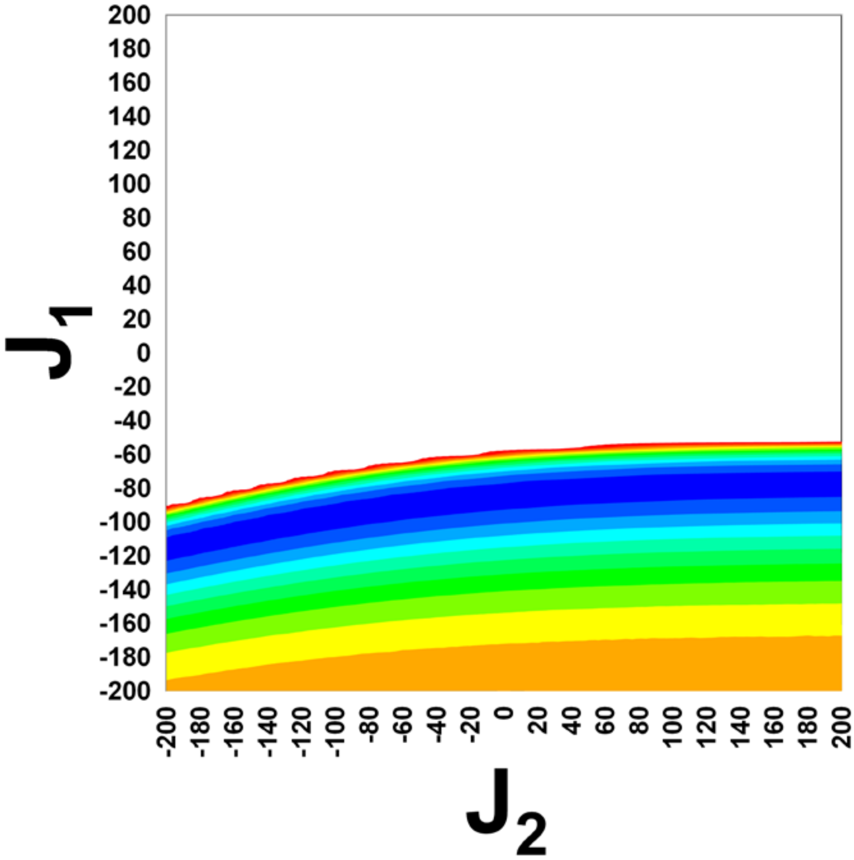

Figure S29. Contour plot of J_1 vs J_2 in cm^{-1} for complex **1** with lowest residual in blue with a fixed value of g = 2.09.

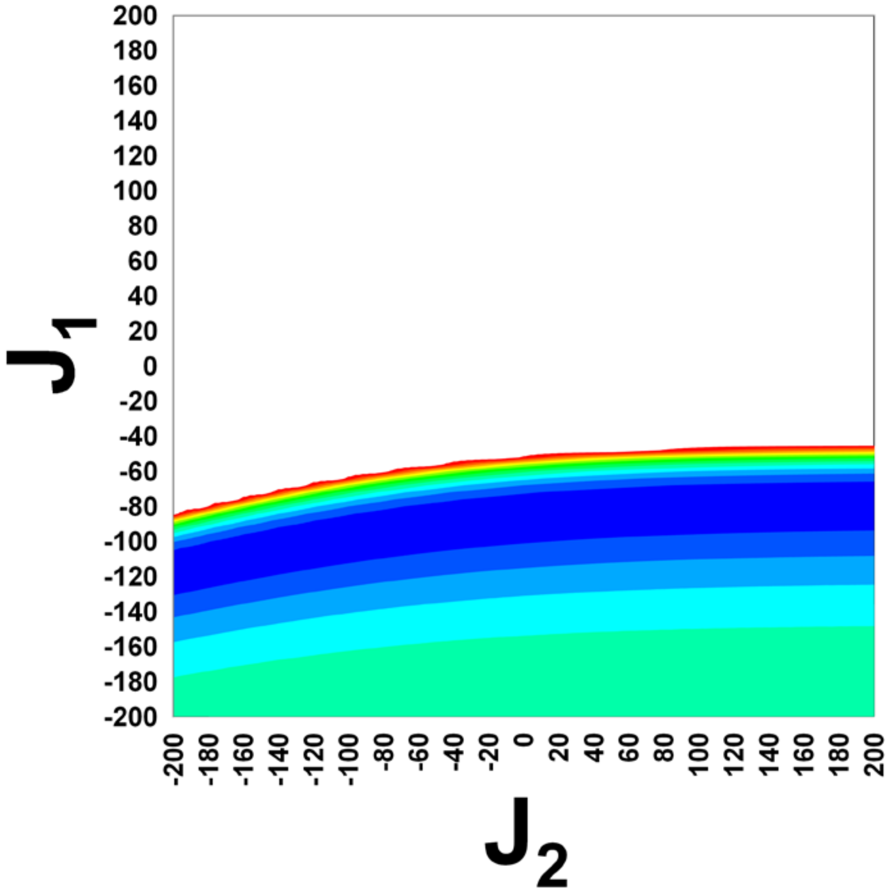

Residual value capped at 3.9.

Figure S30. Contour plot of J_1 vs J_2 in cm^{-1} for complex **1** with lowest residual in blue with a fixed value of g = 2.09. Residual value capped at 7.8.

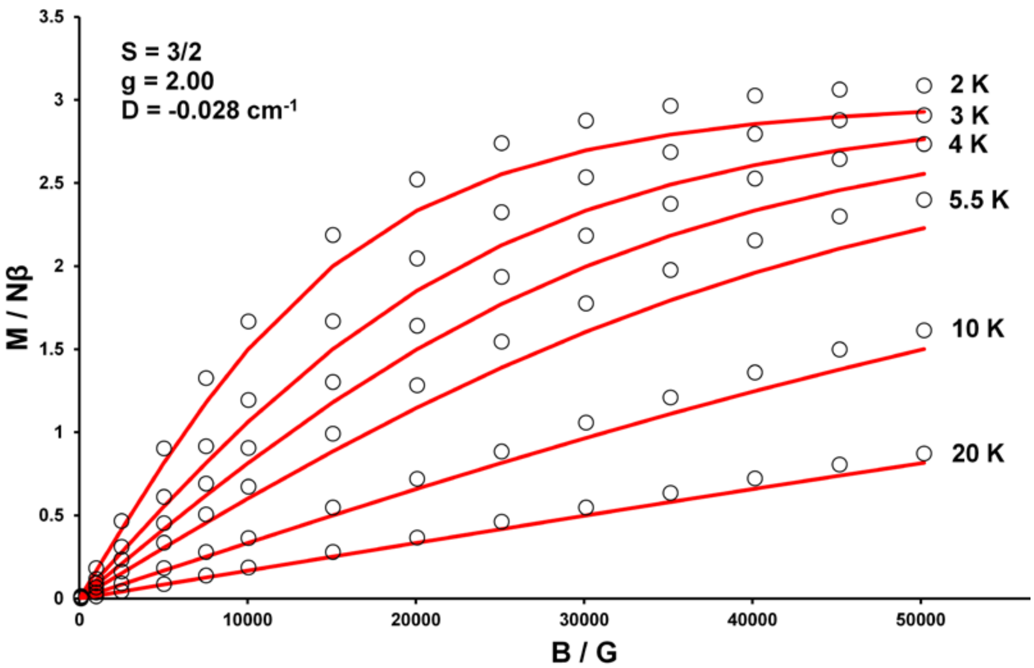

Figure S31. Plot of *M* (*N*β) vs field (0 - 50000 G) for **1** at (top), 3, 4, 5.5, 10 and 20 K (bottom) with g fixed at 2.00 and S = 3/2. The solid red lines represent fits of the experimental data with the parameters shown and in the text.

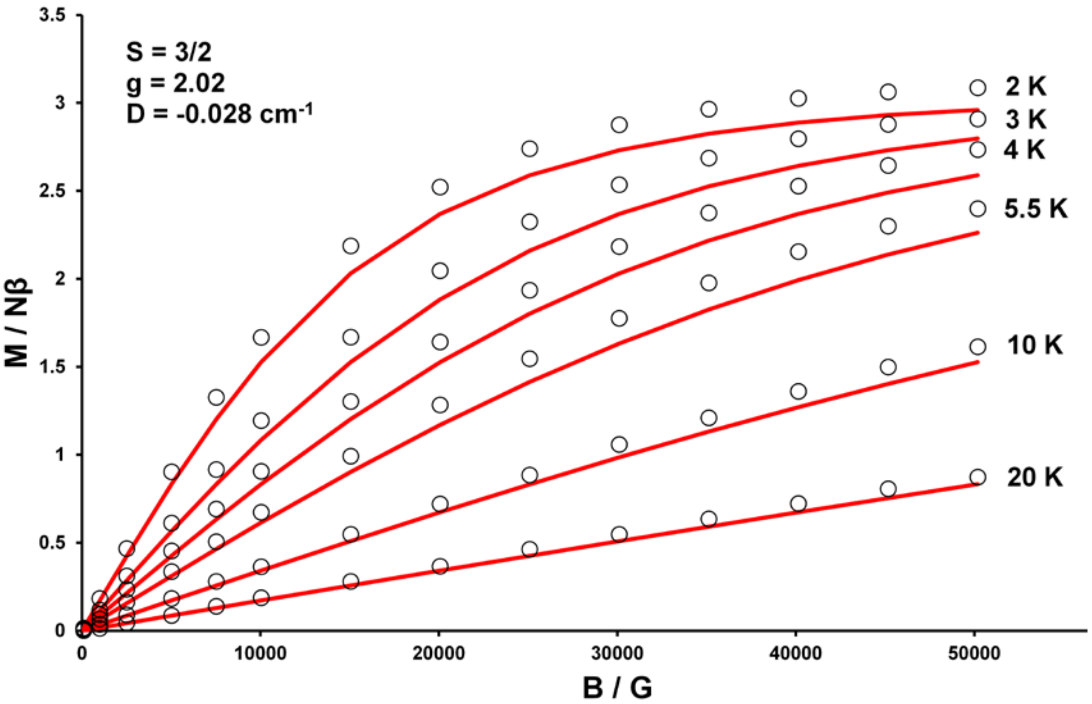

Figure S32. Plot of *M* (*N*β) vs field (0 - 50000 G) for **1** at (top), 3, 4, 5.5, 10 and 20 K (bottom) with g fixed at 2.02 and S = 3/2. The solid red lines represent fits of the experimental data with the parameters shown and in the text.

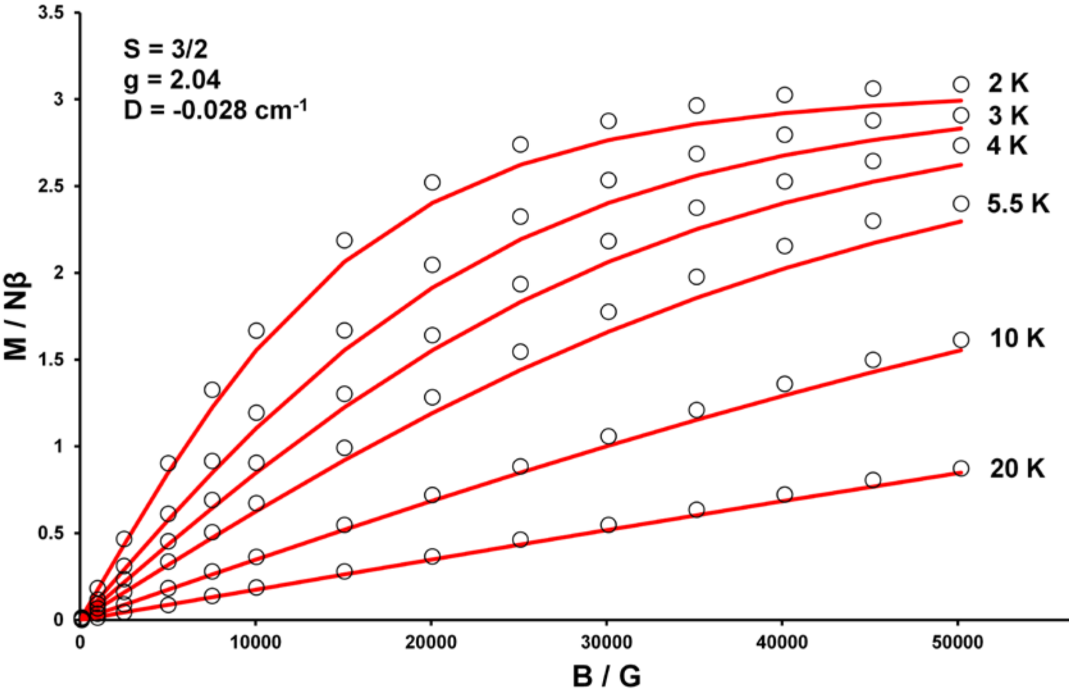

Figure S33. Plot of *M* (*N*β) vs field (0 - 50000 G) for **1** at (top), 3, 4, 5.5, 10 and 20 K (bottom) with g fixed at 2.04 and S = 3/2. The solid red lines represent fits of the experimental data with the parameters shown and in the text.

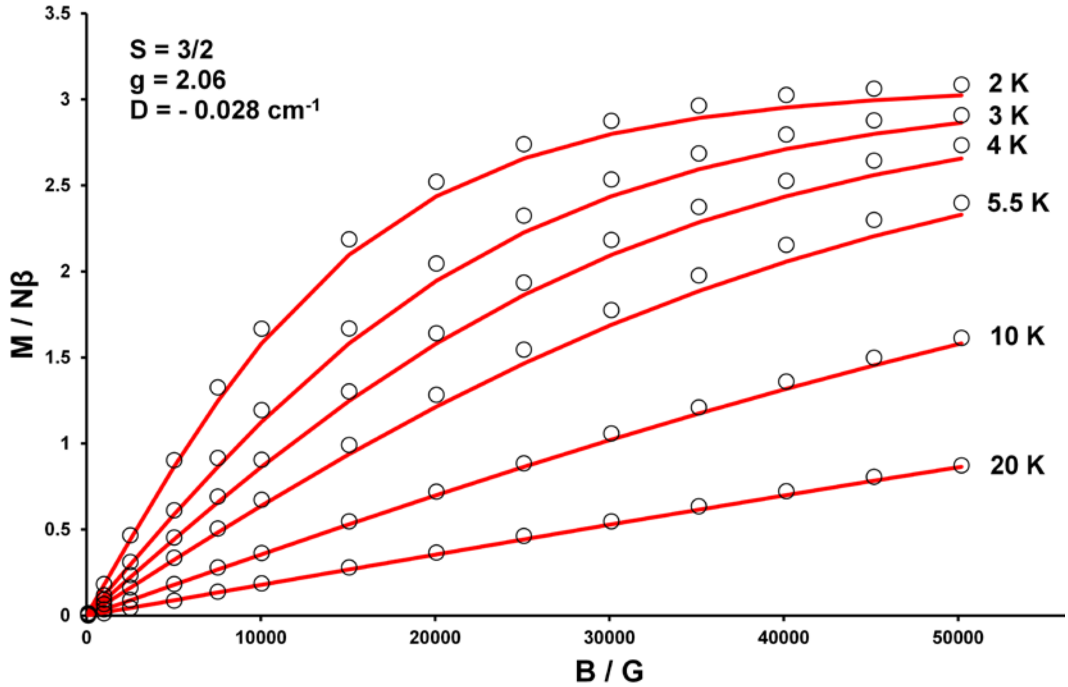

Figure S34. Plot of *M* (*N*β) vs field (0 - 50000 G) for **1** at (top), 3, 4, 5.5, 10 and 20 K (bottom) with g fixed at 2.06 and S = 3/2. The solid red lines represent fits of the experimental data with the parameters shown and in the text.

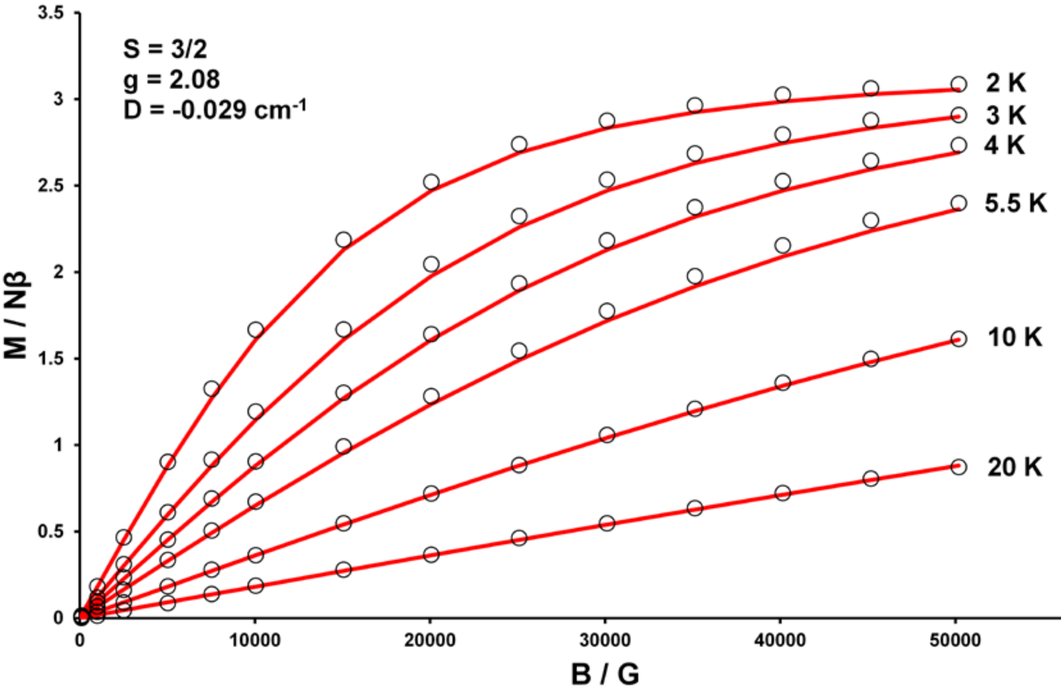

Figure S35. Plot of *M* (*N*β) vs field (0 - 50000 G) for **1** at (top), 3, 4, 5.5, 10 and 20 K (bottom) with g fixed at 2.08 and S = 3/2. The solid red lines represent fits of the experimental data with the parameters shown and in the text.

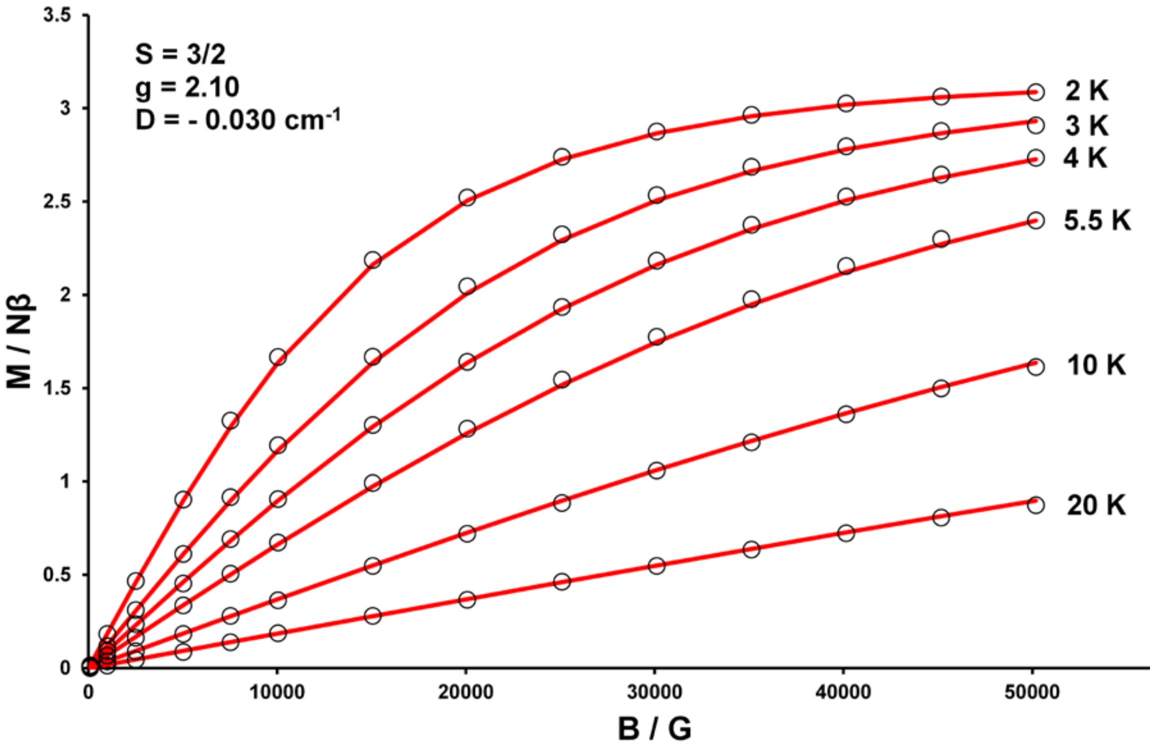

Figure S36. Plot of *M* (*N*β) vs field (0 - 50000 G) for **1** at (top), 3, 4, 5.5, 10 and 20 K (bottom) with g fixed at 2.10 and S = 3/2. The solid red lines represent fits of the experimental data with the parameters shown and in the text.

Table S1 Summary of known mononuclear complexes containing a linear $(L^{\bullet}) - Mn^{II} - (L^{\bullet})$ arrangement and their magnetic data where $L^{\bullet}$ = derivatives of Tempo, Proxyl and Iminoyl / Nitronyl nitroxides.

Formula	Plateaux $\chi_M T$ value ($cm^3\ mol^{-1}\ K$)[a]	J_1 (cm^{-1})[b]	J_2 (cm^{-1})[b]	g	References
$Mn^{II}(hfac)_2(tempo)_2$	1.79	-79	None	1.95	1,2
$Mn^{II}(hfac)_2(proxyl)_2$	1.91	-105	None	2.02	1,2
$Mn^{II}(hfac)_2NITPh$	1.90	-90	None	2.06	3
$Mn^{II}Cl_2(NIT2\text{-}py)_2$	1.84	-79.0	None	1.998	4
$Mn^{II}(4ImNNH)_2(NO_3)_2$	1.80	-97.3	None	1.96	5
$Mn^{II}(4ImNNH)_2(Cl)_2$	1.90	-121.6	None	2.01	5
$Mn^{II}(4ImNNH)_2(Br)_2$	1.80	-108.4	None	1.95	5
$Mn^{II}(hfac)_2(L_1^{\bullet})_2$	2.01	-92.4	None	2.00	6
$Mn^{II}(hfac)_2(L_2^{\bullet})_2$	2.01	-102.2	None	2.00	6
$Mn^{II}(hfac)_2(L_3^{\bullet})_2$	N/A[c]	-311	11.1	2.0 ($L_3^{\bullet}$) 2.14 (Mn(II))	7

Abbreviations: hfac, hexafluoroacetylacetonate; tempo, 2,2,6,6-tetramethylpiperidinyl- 1-oxy; proxyl, 2,2,5,5-tetramethylpyrrolidinyl-l; NITPh, 2-phenyl-4,4,5,5-tetramethyl-4,5-dihydro-1H-imidazolyl-l-oxy 3-oxide; NIT2-py, 2-(2-pyridyl)-4,4,5,5-tetramethyl-4,5-dihydro-1H-imidazolyl-l-oxy 3-oxide; 4ImNNH, (2-(4-imidazolyl)-4,4,5,5-tetramethylimidazolin-1-oxyl 3 oxide; $L_1^{\bullet}$, See Ref 6 (azobenzene tempo derivative); $L_2^{\bullet}$ See Ref 6 (azobenzene derivative); $L_3^{\bullet}$, 1-Iodo-3,5-bis(4´,4´,5´,5´-tetramethyl-4´,5´-dihydro-1H-imidazole-1´-oxyl)benzene.

[a] The values have been converted to $\chi_M T$ units ($cm^3\ mol^{-1}\ K$) and scaled to fit the appropriate spin Hamiltonian : $\hat{H} = -2J_1(\hat{S}_1\hat{S}_2 + \hat{S}_2\hat{S}_3) - 2J_2(\hat{S}_1\hat{S}_3)$ for a clearer comparison.

[b] These values corresponding to fits obtained using the spin Hamiltonian form as above.

[c] The $(L^{\bullet}) - Mn^{II} - (L^{\bullet})$ moiety has an additional two non-interacting iminoylnitroxide radicals and one non interacting Mn(II) ion. The plateaux value in this case is 7.9 $cm^3\ mol^{-1}$ K but has been omitted from the table as it was not a direct comparison.

[1] C. Benelli, D. Gatteschi, C. Zanchini, R. J. Doedens, M. H. Dickman, L. C. Porter, *Inorg. Chem.* **1986**, *25*, 3453. doi: 10.1021/ic00239a027

[2] M. H. Dickman, L. C. Porter, R. J. Doedens, *Inorg. Chem.*, **1986**, *25*, 2595. doi: 10.1021/ic00235a022

[3] A. Caneschi, D. Gatteschi, J. Laugier, L. Pardi, P. Rey, C. Zanchini, *Inorg. Chem.*, **1988**, *27*, 2027. **doi:** 10.1021/ic00285a007

[4] D. Luneau, G. Risoan, P. Rey, A. Grand, A. Caneschi, D. Gatteschi, J. Laugier, *Inorg. Chem.*, **1993**, *32*, 5616. **doi:** 10.1021/ic00076a032

[5] C. Aoki, T. Ishida, T. Nogami, *Inorg. Chem.*, **2003**, *42*, 7616. **doi:** 10.1021/ic0349048

[6] M. Fujino, S. Hasegawa, H. Akutsu, J. Yamada, S. Nakatsuji, *Polyhedron*, **2007**, *26*, 1989. doi:10.1016/j.poly.2006.09.050

[7] M. G. V. Vaz, H. Akpinar, G. P. Guedes, S. Santos-Jr, M. A. Novak, P. M. Lahti, *New. J. Chem.*, **2013**, 37, 1927. doi: 10.1039/c3nj00047h